Profiling atmospheric water vapor using a fiber laser lidar system

Russell J. De Young[1,*] and Norman P. Barnes[2]

[1]Sciece Directorate, NASA Langley Research Center, MS401A, Hampton, Virginia 23681, USA

[2]Systems Engineering Directorate, NASA Langley Research Center, MS474, Hampton, Virginia 23681, USA

*Corresponding author: russell.j.deyoung@nasa.gov

Received 19 November 2009; accepted 16 December 2009;
posted 7 January 2010 (Doc. ID 120204); published 21 January 2010

A compact, lightweight, and efficient fiber laser lidar system has been developed to measure water vapor profiles in the lower atmosphere of Earth or Mars. The line narrowed laser consist of a Tm:germanate fiber pumped by two 792 nm diode arrays. The fiber laser transmits ~0.5 mJ Q- switched pulses at 5 Hz and can be tuned to water vapor lines near 1.94 μm with linewidth of ~20 pm. A lightweight lidar receiver telescope was constructed of carbon epoxy fiber with a 30 cm Fresnel lens and an advanced HgCdTe APD detector. This system has made preliminary atmospheric measurements.

OCIS codes: 010.3640, 060.2320, 060.3510, 120.0280, 140.3600, 280.1910.

1. Introduction

Water vapor is the most radiatively active gas in the atmosphere, both capturing and transporting energy within the atmosphere. This influences weather patterns and ultimately climate. The concentration of water vapor is highly variable in both time and space. It primarily resides in the boundary layer, therefore making measurements of concentration difficult. Nevertheless, to predict future weather with meaningful accuracy, a multitude of real time measurements of water vapor need to be taken as a function of altitude. These data serve as input for atmospheric models to accurately predict weather resulting in major economic consequences.

Weather stations would include a water vapor lidar, which would continuously determine the water vapor vertical atmosphere concentration in the vicinity of the station. Lidar can not only give the water vapor concentration but also measure aerosol profiles and cloud and boundary layer heights. These data are valuable weather model inputs. Such a lidar would employ the differential absorption lidar (DIAL) technique [1]. There are a plethora of water vapor absorption lines that could be employed. However, it is prudent to employ wavelengths in the eye-safe region of the spectrum to avoid interference with aircraft.

This same technology could be employed on Mars to determine atmospheric water vapor profiles. Although the concentration of water vapor is very low, there is still sufficient vapor to form hazes, ground fog, frost, and clouds. An exchange of water vapor exists between the ice cap at the Northern pole and the atmosphere. The ice cap grows and recedes with the seasons. There is long term interest in the question of whether life exists on Mars today in any form. Life as known on planet Earth requires water. Thus, there is great interest in determining the concentration and extent of present day water on the Martian surface and atmosphere. The DIAL technique could be utilized to measure the processes that determine the distribution of water vapor and thus indicate where sources and sinks of water vapor exist. This could then lead to sites where life on Mars might be found.

Remote sensing of water vapor in the atmosphere of Mars and Earth can be accomplished by employing the DIAL lidar technique. This requires a laser that

0003-6935/10/040562-06$15.00/0

is tunable around a strong water vapor absorption feature. The DIAL lidar transmits a pair of laser pulses. The first pulse is tuned to the peak of the absorption feature, and the second laser pulse is tuned to a wavelength well away from the water vapor absorption feature. Aerosol particles in the atmosphere scatter some of the transmitted laser pulse back to the DIAL receiver. Water vapor concentration can be determined as a function of altitude by taking the logarithm of the ratio of the backscattered returns. Measurements under arid atmospheric conditions or measurements over short ranges benefit by probing very strong water vapor absorption features. Such absorption features are found in the vicinity of 1.9 μm. Because these absorption features are narrow, the laser spectral bandwidth must be much narrower than the water vapor absorption features. For best results, the pair of laser pulses should be in close temporal proximity in order to probe the same volume of the atmosphere. For short ranges, only a modest amount of laser energy is required. However, for good range resolved measurements, the Q-switched pulse length should be short, less than 100 ns.

Both the Earth and Mars applications require a laser system that is rugged, dependable, lightweight, efficient, and with a long service lifetime. A narrow line, tunable, efficient fiber laser could fulfill the challenging conditions demanded by these applications. Such a laser would need a narrow linewidth, be rapidly tunable to the peak of a strong water vapor absorption line and then off that line, have high pulse repetition frequency (for signal averaging), be highly efficient and low mass especially for the Mars application, and be rugged for deployment in autonomous, remote locations. Fiber lasers have advanced to the point that they are potential candidates for use in lidar systems that can be deployed easily and at low cost for atmospheric profiling applications.

This paper describes a Tm:germanate fiber laser, tunable around 1.9 μm, coupled to a low mass lidar receiver that can fulfill the above requirements for a water vapor DIAL system. To demonstrate the applicability of Tm:germanate for remote sensing, this material was fabricated into a double clad fiber laser and diode pumped. Spectroscopic parameters of Tm:germanate have been measured [2,3]. The selection of Tm:germanate was dictated by reliability, efficiency, and tuning considerations.

To be efficient, a diode pumped laser should have a quantum efficiency approaching 2.0 when pumped at 0.79 μm. An energy level diagram of Tm appears in Fig. 1. High power laser diodes are commercially available to pump the $^3H_4$ manifold. If a single pump photon produces a single active atom in the upper laser manifold, the laser efficiency is then limited by a ratio of photon energies, λ_P/λ_L. If commercially available laser diodes at ≈0.79 μm are employed for pumping, this ratio is ≈0.4. Fortunately, self-quenching can increase this efficiency significantly. Through the self-quenching process, a Tm atom in the $^3H_4$ manifold can interact with a nearby Tm atom in the $^3H_6$ manifold to transfer both Tm atoms into the $^3F_4$ manifold, the upper laser manifold. This process is in competition with natural decay of the $^3H_4$ manifold. Natural decay of the $^3H_4$ manifold is a result of both radiative and nonradiative transitions, however, nonradiative transitions are usually dominant. When self-quenching is competitive, the laser efficiency becomes $\eta_Q\lambda_P/\lambda_L$. The quantum efficiency, η_Q, is the average number of Tm atoms promoted to the $^3F_4$ manifold for each absorbed photon. In an ideal circumstance, the quantum efficiency approaches 2.0.

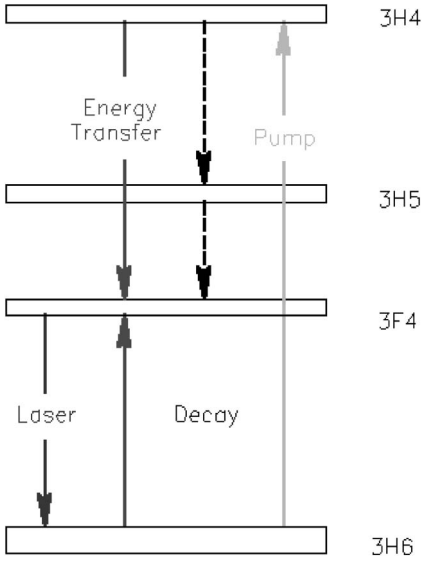

Fig. 1. Energy manifolds of Tm.

Nonradiative transitions can be minimized by a judicious choice of laser material. Nonradiative transitions require the emission of phonons so that energy is conserved. The required number of phonons is approximately the energy gap to the next lower manifold divided by the maximum phonon energy. As a rule of thumb, if the required number of phonons is ≈5 or greater, nonradiative transitions will not be competitive. The energy gap between the $^3H_4$ and $^3H_5$ manifolds is approximately 4500 cm^{-1}. Thus, the maximum phonon energy of the selected laser material should be less than 900 cm^{-1}. Maximum phonon energy of germanate glasses were found to be in the range of 800 to 975 cm^{-1} [3] by looking at high lying levels. Similar results were found for GeO_2—Na_2O glasses and lower phonon energy for GeO_2—Cs_2O. For comparison, the maximum phonon energy of silica and ZBLAN is approximately 1100 and 500 cm^{-1}, respectively. From a phonon energy point of view, germanate and ZBLAN laser materials are favored. However, ZBLAN is not a physically robust material and this militates against its use in physically demanding applications.

2. Experimental Setup

A photo and schematic diagram of the Tm:germanate fiber laser is shown in Fig. 2. The fiber is doped with

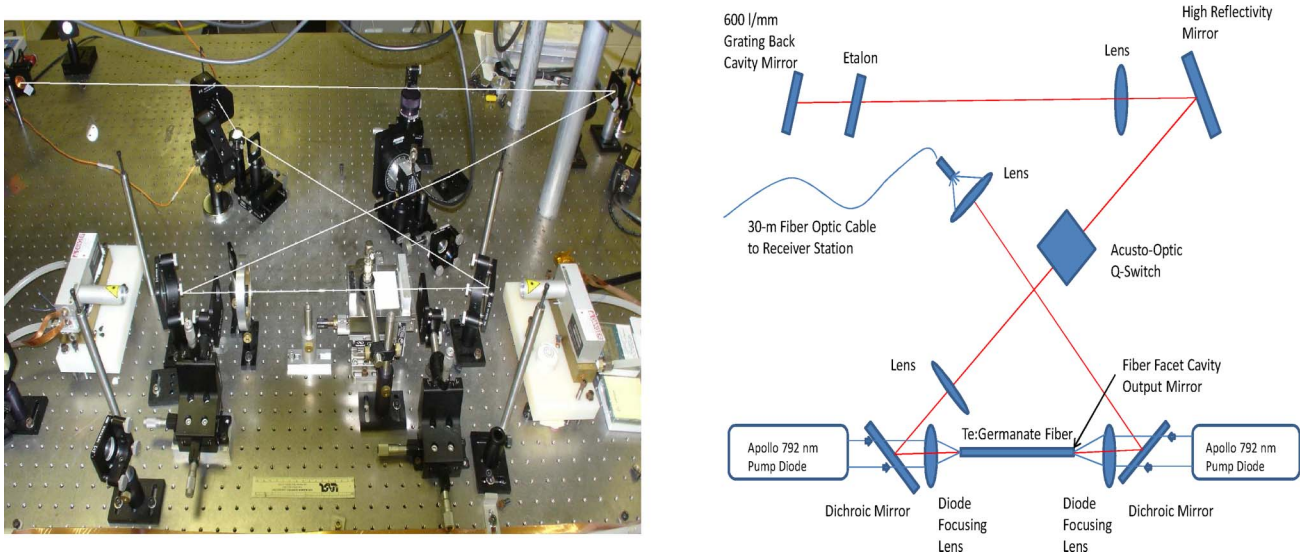

Fig. 2. (Color online) Schematic and photo of the Tm:germanate fiber laser transmitter.

4% Tm and has a core diameter of 35 μm. The fiber length is 35 cm and is pumped with two 0.792 μm diodes (Apollo Instruments, Inc. C25-792-0PH, 25 W) that are focused onto the fiber inner cladding with a pair of lenses. Dichroic mirrors allow the pump radiation to be transmitted to the fiber but reflect the infrared laser radiation. The laser resonator consists of the partial reflecting fiber facet and the highly reflective 600 lines/mm grating. The cavity is long to allow the beam to expand and fill the grating, thus line narrowing the laser emission. A 0.2 mm thick, fused silica etalon is used to further reduce the laser linewidth to approximately 20 pm (measured by an infrared wavemeter), which was well within the pressure broadened on-line width of 63 pm. An acusto-optic Q-switch allows the resonator to be pulsed, resulting in typically 5 Hz pulses of 110 ns pulse length. The output from the fiber facet is then focused into a 30 m long, 50 μm core, 0.22 NA step index multimode fiber (AFS50/125Y ThorLabs). This fiber allowed the pulsed laser radiation to be directed out of the laboratory building and into the atmosphere for testing. The energy out of the fiber to laser energy incident on the fiber was typically 40%.

Wavelength tuning was accomplished by rotating the grating to the water vapor absorption feature of interest and then rotating the etalon so that a mode of the etalon was near the peak of the grating reflection. The wavelength and linewidth could be constantly monitored by the interferometer. There are numerous water vapor lines of sufficient absorption strength in the 1.94 μm region as shown in Fig. 3 [4]. The DIAL on-line wavelength was chosen to be the 1.94301 μm line, and the off line was chosen to be in the water vapor free region at 1.94246 μm.

3. Experimental Results

Figure 4 shows the 5 Hz Q-switched laser output as a function of pump diode current for the on-line (1.94301 μm) and off-line (1.94265 μm) DIAL wavelengths. Note that the on-line wavelength experiences more absorption that the off-line, as expected. This is

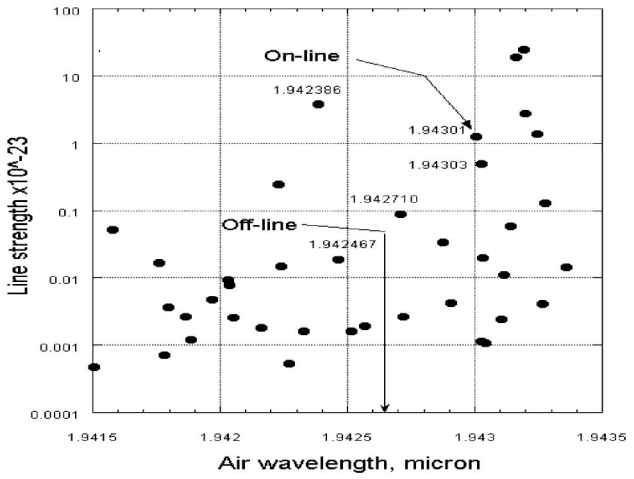

Fig. 3. Line strength of water vapor lines near 1.94 μm. The on- and off-line wavelengths are indicated.

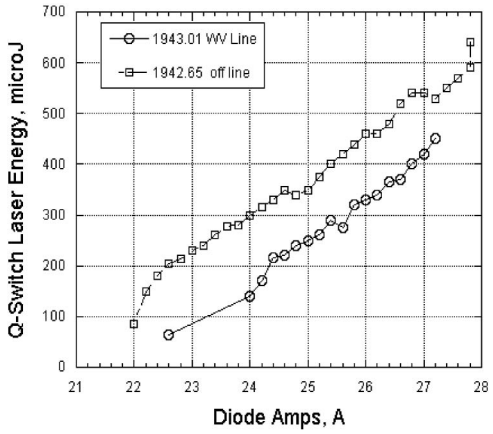

Fig. 4. Pulsed laser output versus pump diode current.

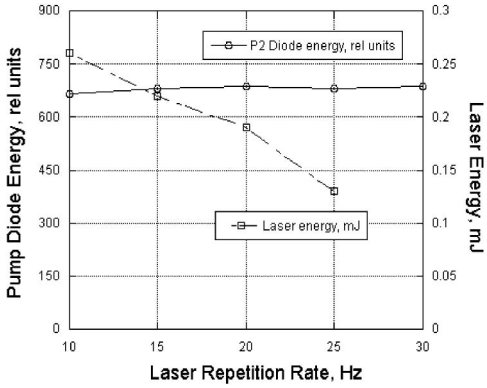

Fig. 5. Pump diode optical energy and pulsed laser output energy versus pulse repetition frequency.

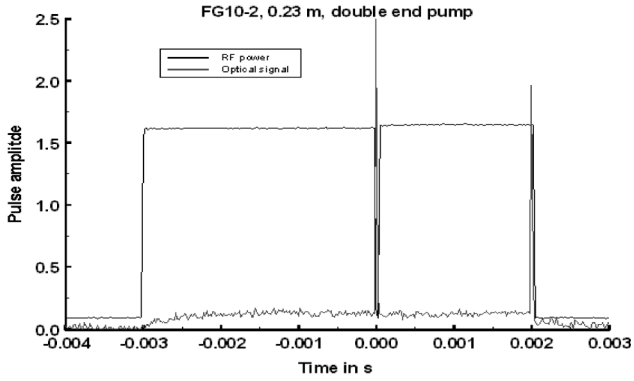

Fig. 7. Demonstration of two Q-switched pulses from a single diode pump pulse.

a result of the long laser resonator length, which was exposed to ambient air. The laser would stay within 20 pm of the on-line wavelength over a period of 10–20 min but would tend to drift after that period due to laboratory room temperature changes. As the wavelength drifts, the water vapor absorption changes and must be recalculated for wavelengths other than the center of the on-line wavelength. In the future the laser will need to be placed in a temperature controlled enclosure. Pulsed energies exceeding 0.5 mJ are possible without fiber facet damage.

The laser was typically pulsed at a pulse repetition frequency of 5 Hz, but higher rates are advantageous for averaging the atmospheric lidar signal for noise reduction. Figure 5 shows the pump diode energy and the 1.94 μm laser output energy as a function of the laser pulse repetition frequency. As seen in the figure the laser energy decreases as the pulse repetition frequency increases. However, the pump diode optical energy remains constant, indicating that the fiber is becoming less efficient probably due to heating. Heating increases the population density of the lower laser level of this quasi-4-level laser. Future modifications will incorporate a cooled metal plate rather than having the fiber cooled by ambient air only.

Figure 6 shows the effect of increased diode pump energy on the Q-switched energy and pulse length. As the pump power increases, the laser output energy increases but the laser pulse length decreases. Nominal pulse energies were 0.3 mJ with a pulse length of 140 ns.

One useful feature of the fiber laser system is the ability to obtain two Q-switched pulses from the fiber during one diode pump pulse. This is demonstrated in Fig. 7, where the radio frequency energy is rapidly turned off twice during the diode pump pulse. The Q-switch is turned off once during the pump pulse and again at the end of the pump pulse. This results in the laser resonator returning to a high Q condition thus producing the two Q-switched pulses as shown. Although the second pulse, delayed by 2 ms, is somewhat lower in energy, it still has sufficient energy to be useful. By adjusting the time when the Q-switch is turned off during the pump pulse, the two pulses can be made to have equal energy. Such pulsing is useful when the laser resonator can be tuned rapidly between the on- and off-line wavelengths. This allows a very short time interval between atmospheric on- and off-line returns, thus measuring a water vapor profile with little change in atmospheric conditions.

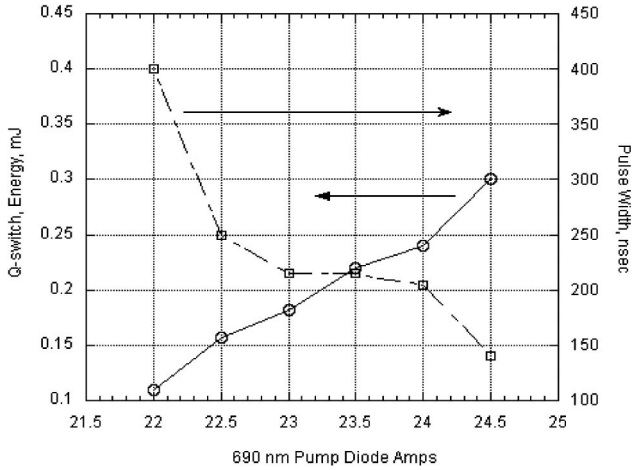

Fig. 6. Q-switched laser output energy and pulse length versus pump diode current in amperes.

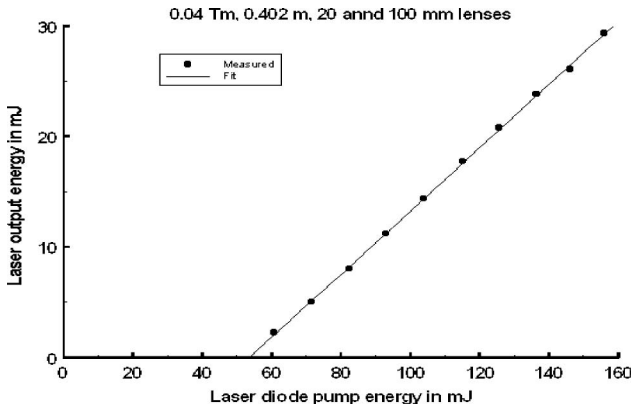

Fig. 8. Normal mode laser energy out versus pump diode input energy demonstrating a slope efficiency of 0.28 and an inferred quantum efficiency of 1.75.

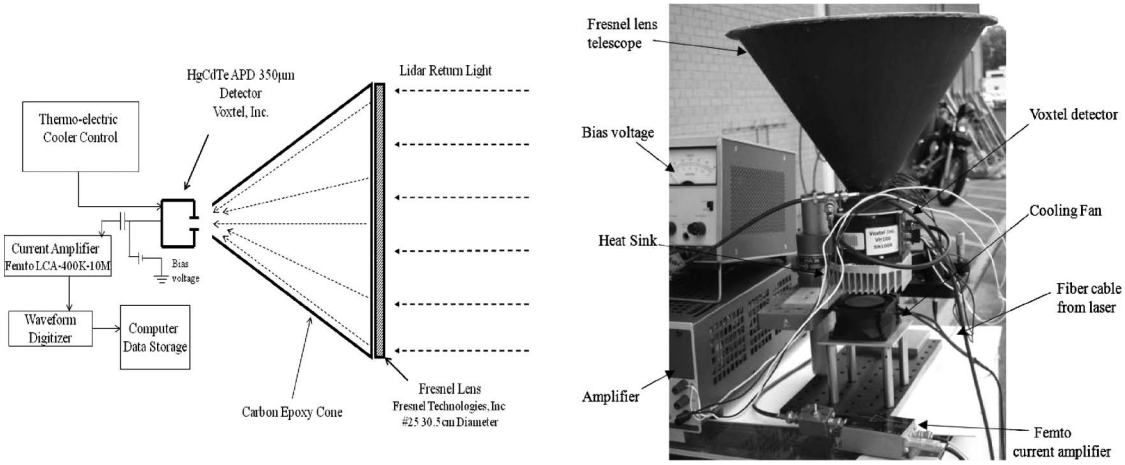

Fig. 9. Schematic diagram and photo of the lidar receiver system.

Figure 8 demonstrates the normal mode laser output at 1.94 μm. as a function of diode pump energy in mJ. This results in a slope efficiency of 0.28 and infers a quantum efficiency of 1.75 in close agreement with the maximum theoretical quantum efficiency of 2. The diode electrical to optical efficiency is 0.5 and coupled with a laser slope efficiency of 0.28 results in a total slope efficiency of 0.14 for normal mode lasing. Slope efficiency is somewhat lower for Q-switched lasing. Improvements in efficiency could be made by reducing resonator losses and improving diode to fiber coupling efficiency. Nevertheless, this laser can easily operate above 0.10 efficiency.

4. Lidar Receiver System

The lidar receiver consists of a plastic 30 cm diameter Fresnel lens (213 mm F.L., 2 grooves/mm) that has 85% transmission at 2 μm and is shown in Fig. 9. This lens was glued to a carbon fiber epoxy cone, providing a rigid telescope structure. A 350 μm diameter HgCdTe avalanche photodiode detector (Voxtel, Inc.) was adjusted to the focal point of the Fresnel lens, the resulting field-of-view was 1.6 mrad [5,6]. A 1.94048 μm filter (70% T, 10.52 nm FWHM, Andover) could be placed in front of the detector when needed to block the solar input. The detector has a thermoelectric cooler to lower the detector temperature to 239 K. The bias voltage can be adjusted to provide detector gain which for a maximum voltage of 18 V was 50 at 239 K. The output of the detector was capacitively coupled to a current amplifier (Femto LCA-400K-10M) then to a 12 bit waveform digitizer that averaged the lidar returns and stored the results on a laptop computer. This receiver is very lightweight, compact, and suitable for deployment at remote locations.

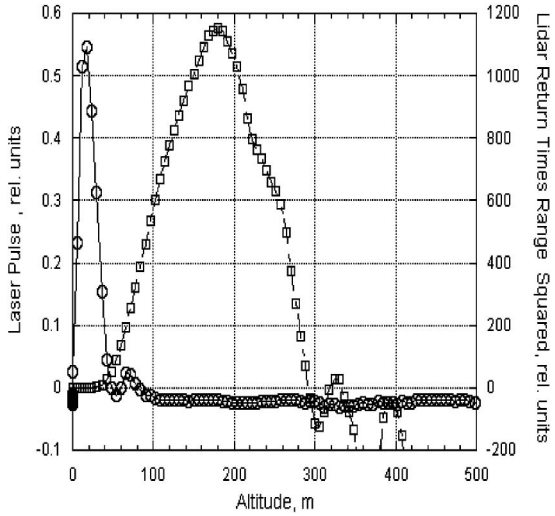

Fig. 10. Plot of atmospheric lidar return and the corresponding laser pulse entering the atmosphere.

This receiver was used to make preliminary atmospheric lidar measurements. The 30 m fiber cable was routed out of the laboratory to the outside of the laboratory building. It was attached to a beam-expanding telescope consisting of a 25.4 mm focal length lens resulting in a ~1.5 mm diameter beam. When correctly adjusted, the beam divergence was ~1.0 mrad, slightly less than the telescope field-of-view of 1.6 mrad.

The laser transmitted energy was low at approximately 50 μJ. The pulse repetition frequency was 5 Hz, and the lidar return signal was averaged for 100 shots. Figure 10 shows the laser pulse exiting the fiber and the corresponding atmospheric range squared lidar return at the off-line wavelength. The laser pulse exits the beam expander telescope and enters the atmosphere. The corresponding lidar return is seen after the laser pulse and continues to rise as the laser pulse enters the telescope field-of-view. At 180 m the laser beam is fully in the telescope field-of-view, and thereafter the receiver records the atmospheric scattering until 300 m where the return signal equals the system noise. By increasing the laser energy substantially greater altitude returns can be recorded.

5. Conclusion

A new compact, efficient, and lightweight water vapor lidar system has been constructed to measure the

atmospheric water vapor profile from Earth or Mars surface. The laser transmitter uses a Q-switched Tm: germanate fiber lasing at $\sim 1.9\,\mu$m producing typically 0.5 mJ pulses at 5 Hz. The fiber is pumped by two 792 nm diode arrays, entering the fiber from either end. The linewidth is narrowed to ~ 20 pm by use of a grating and etalon and the laser is tuned to the "on-line" and "off-line" wavelengths by adjusting the grating. The fiber laser could produce two Q-switched pulses from a single diode pump pulse, resulting in two closely timed DIAL pulses. Normal mode laser efficiency was measured to be 14%.

A low mass lidar receiver was constructed of carbon fiber epoxy using a 30 cm diameter plastic Fresnel lens. A HgCdTe detector was used to detect the atmospheric "off-line" backscatter return. Future measurements will transmit at both the "on-line" and "off-line" wavelengths and then using the DIAL technique result in the atmospheric water vapor profile. Such a lidar would then be used at multiple Earth locations to accurately measure the water vapor profile for improved weather predictions and also on Mars to determine the location of sources and sinks of water vapor to derive possible locations of life on Mars.

References

1. C. Weitkamp, ed., *LIDAR Range-Resolved Optical Remote Sensing of the Atmosphere* (Springer, 2005).
2. B. M. Walsh, N. P. Barnes, D. J. Reichle, and S. Jiang, "Optical properties of Tm3+ ions in alkali germanate glass," J. Non-Cryst. Solids **352**, 5344–5352 (2006).
3. N. P. Barnes, B. M. Walsh, D. J. Reichle, R. J. DeYoung, and S. Jiang, "Tm:germanate fiber laser: tuning and Q-switching," Appl. Phys. B **89** 299–304 (2007).
4. The hitran database, http://www.hitran.com.
5. G. M. Williams, M. A. Compton, and A. S. Huntington, "High-speed photon counting with linear-mode APD receivers," Proc. SPIE **7320**, 732012 (2009).
6. M. B. Reine, J. W. Marciniec, K. K. Wong, T. Parodos, J. D. Mullarkey, P. A. Lamarre, S. P. Tobin, K. A. Gustavsen, and G. M. Williams, "HgCdTe MWIR back-illuminated electron-initiated avalanche photodiode arrays," SPIE Optics and Photonics Meeting, San Diego, California, 13–17 August, 2006.